Synthesis and characterization of starch sulfates obtained by the sulfamic acid-urea complex

Feride Akman[1], Alexandr S. Kazachenko[2*] 0000-0002-3121-1666**, Natalya Yu. Vasilyeva[2,3], Yuriy N. Malyar[2,3]** 0000-0001-9380-0290

[1] University of Bingöl, Vocational School of Technical Sciences, 12000 Bingöl, Turkey

[2]Institute of Chemistry and Chemical Technology SB RAS, Federal Research Center "Krasnoyarsk Science Center SB RAS", Akademgorodok, 50/24, Krasnoyarsk, 660036, Russia

[3] Siberian Federal University, Svobodny av., 79, Krasnoyarsk, 660041, Russia

[*]Corresponding author, Aleksandr Kazachenko e-mail: leo_lion_leo@mail.ru

Received [Dates will be filled in by the Editorial office]

Abstract

The process of solid-phase sulfation of starch with sulfamic acid in the presence of urea was studied. The sulfur content of starch sulfate increases with increasing sulfation temperature from 70 to 100 ° C. To obtain starch sulfates with a high sulfur content (about 10 wt.%), It is advisable to carry out the sulfation process at a temperature of 100 ° C for 120 minutes. Mathematical modeling of the process of solid-phase sulfation of starch with sulfamic acid in the presence of urea was carried out. The introduction of a sulfate group in the structure of starch is confirmed by FTIR spectroscopy. In the FTIR spectra of sulfated starch, in contrast to the original starch, there are absorption bands at 1255 cm^{-1}, 808-817 cm^{-1} and 859-867 cm^{-1}, corresponding to sulfate groups. Solid-phase sulfation of starch with a complex of sulfamic acid - urea can improve the environmental safety and efficiency of the process in comparison with the known methods of sulfation. Initial starch and sulfated starch were analyzed by gel permeation chromatography. The initial starch was shown to have a main peak with Mn 139 kDa and Mw 382 kDa, and sulfated starch has a peak in the chromatogram relating to Mn 44 kDa and Mw 60 kDa. Besides, the quantum chemical calculations of the starch and sulfated starches (in dimer forms) formed when different number of hydroxyl groups in starch were replaced with sulfate groups were performed using the DFT/B3LYP method with 6-31+G (d, p) basis set in the ground state. Firstly, these molecules were optimized. Then, from the optimized geometry of the starch and sulfated starches, frontier molecular orbitals (FMOs), molecular electrostatic potential (MEP) surfaces, bond parameters, chemical reactivity descriptors such as chemical potential, electron affinity, electronegativity, ionization energy, electrophilicity index and chemical hardness have been calculated theoretically. In addition, spectroscopic analyzes of starch and sulfated starches such as FTIR and ^{1}H NMR were theoretically performed using the same method and compared with each other.

Keywords: starch, sulfation, sulfamic acid, sulfated starch, DFT, HOMO-LUMO, MEP solid-phase synthesis, structure.

Introduction

Polysaccharides are the most abundant polymer on Earth. They are present in both plants, animals and microorganisms. Polysaccharides are long-chain polymers of mono-, di- and oligosugars linked by glycosidic bonds [1,2]. It is known that the introduction of a sulfate group in the structure of a polysaccharide can give them anticoagulant, antioxidant, antiviral and anti-inflammatory activity [1].

Due to their biological activity, sulfated polysaccharides are increasingly being studied as antithrombotic agents and anticoagulants as an alternative to heparin. Heparin is actively used in clinical practice. It is obtained from raw materials of animal origin, however, it can cause negative side effects on the human body and be a source of pathogenic microflora [3].

Polysaccharides can be chemically modified with sulfate groups, which can improve and also give them new biological properties. The biological activity of sulfated polysaccharides also depends on their molecular weight [3,4]. Complexes of sulfuric anhydride with various basic reagents have been widely used for sulfating polysaccharides. This method is widely used with minor modifications to sulfate many carbohydrates and related compounds [3,5-8].

Among the many polysaccharides, starch is widely used - a polymer consisting of glucose units connected by glycosidic bonds [9]. In industry, starch is used as a thickener, viscogen, binding agent and carrier of active substances. Chemical modification of starch by sulfate groups can enhance the biological activity, giving it anticoagulant, hypolipidemic and antiviral properties [10]. It was shown in [11,12] that with increasing sulfur content in starch sulfate, its anticoagulant activity increases. Sulfated starch also can be used as a plasticizer for hydraulic binders, thermoset food adhesives, protective colloids, a thickener for food products and drilling fluids, coatings for paper and textiles [13].

Currently, there are several methods for producing sulfated starch. Traditionally, starch sulfates are produced using highly hydrolytic sulfating agents, such as sulfuric acid, chlorosulfonic acid and sulfur trioxide [14-16]. The use of these sulfating agents can lead to hydrolysis or decomposition of starch chains during the [17,18]. To reduce the hydrolytic or degrading effect, various organic solvents, such as pyridine, dimethyl sulfoxide, triethylamine, toluene, or ethylene dichloride, was used as the reaction medium [19-22]. Thus, it becomes relevant to develop starch sulfation methods using more environmentally friendly methods without the use of toxic solvents.

The aim of this work was an environmentally more secure solid-state synthesis of starch sulfates using the sulfamic acid-urea complex and their study by FTIR spectroscopy, DFT method, and gel permeation chromatography.

Experimental

As the source of raw materials are used potato starch (LLC "Nsk-st").

Sulfation of starch was carried out by the sulfamic acid-urea complex according to a modified procedure [23]. To do this, the sulfating complex (SC) and starch were triturated to obtain a homogeneous mass. Sulphating complex was obtained by preliminary mixing 7.2 g of sulfamic acid (75 mmol) and 4.5 g of urea (75 mmol). The ratio of starch and sulfating complex was 1: 3 (mol / mol). The resulting reaction mixture was thermostated with constant stirring and at temperatures of 70, 80, 90 and 100 ° C, with a process duration of 30, 60, 120 and 180 minutes. In this temperature range, the reaction mass melted.

At the end of the thermostating process, the melt was cooled to room temperature, the formed solid product was dissolved in 50 ml of water, the unreacted sulfamic acid was neutralized with a 10% aqueous sodium hydroxide solution to pH 7-8. The resulting solution was evaporated to a volume of 10-15 ml in vacuum of a water-jet pump.

Purification of the sodium salt of sulfated starch was carried out by dialysis on cellophane against distilled water. The product was dialyzed for 10 hours, changing the water at intervals of 1-2 hours.

The FTIR spectra of initial starch and sulfated starch were recorded using a Tensor-27 FTIR spectrometer (Bruker, Germany) within the wavelength range of 400–4000cm^{-1}. The spectral information was analysed using the OPUS program (version 5.0). Solid samples for analysis were prepared in the form of pills in a KBr matrix (2 mg sample/1000 mg KBr).

The average molecular weight (Mw), average molecular mass (Mn) and polydispersity of sulfated starch samples were defined by gel permeation chromatography using an Agilent 1260 Infinity II Multi-Detector GPC/SEC System chromatograph with triple detection: by a refractometer (RI), by a viscometer (VS) and by a light scattering (LS). The separation was made on two Aquagel-OH Mixed-M columns using the solution 0.2M$NaNO_3$ + 0,01MNaH_2PO_4 in water (pH = 7) as the mobile phase. The column was calibrated using polydisperse polyethylene glycol standards (Agilent, USA). The feed rate of the eluent was 1 ml / min, the volume of the used sample was 100 μl. Before analysis, the samples were dissolved in the mobile phase (1 mg / ml) and filtered through a 0.45 μm PTFE membrane

filter (Millipore). Data collection and data processing were performed using Agilent GPC / SEC MDS software.

Elemental analysis of sulfated starch was performed on a FlashEA-1112 elemental analyzer (ThermoQuest, Italia).

Calculation of kinetic data was performed as described in [24]. The numerical optimization of the starch sulfation process with sulfamic acid was carried out using the Statgraphics Centurion XVI software, according to the procedure described in [25].

Computational methods

The quantum chemical calculations have been performed to optimize the starch (a) and sulfated starches such as Sulfated Starch (b) (C7 and C17), Sulfated Starch (c) (C6,C7 and C16,C17) and Sulfated Starch (d) (C1,C6,C7 and C11,C16,C17) (in dimer forms) using Density Functional Theories (DFT)/B3LYP which is Becke's [26] three parameter hybrid exchange functional with Lee-Yang-Parr correlation functional [27] method with 6-31+G (d,p) basis set using Gaussian 09 W software [28]. The HOMO and LUMO plots, MEP and contour maps and the optimized molecular structures were visualized using GaussView 05 program [29]. Also, the chemical shifts (^{1}H NMR) which were calculated using the GIAO (gauge-including atomic orbital) method [30,31] using D_2O solvent, electronic properties, molecular structure parameters and vibrational frequencies of the the starch and sulfated starches (in dimer form) were calculated.

Results and discussion

1. Features of the process of solid-phase sulfation of starch with sulfamic acid-urea complex

Starch sulfation reaction with sulfamic acid-urea complex and the subsequent isolation of starch sulfate in the sodium salt form was carried out according to the scheme:

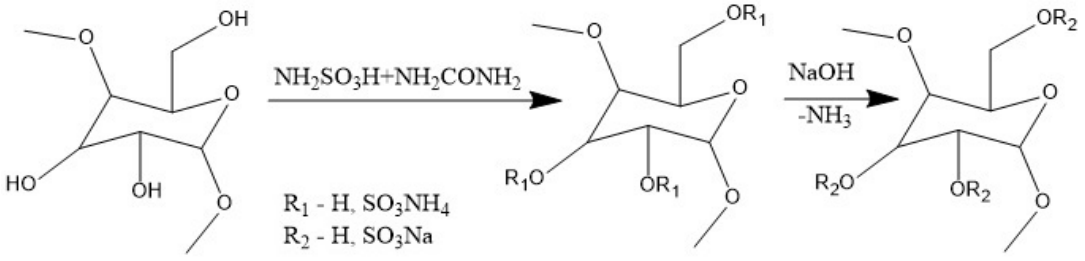

The mechanism of sulfation of polysaccharides by sulfamic acid is not well understood. However, it is assumed [32-35] that upon alcohols sulfation reaction proceeds by

the first order for sulfamic acid and zero order for alcohol. This shows that the limiting stage is some kind of transformation in the acid molecule, possibly its decomposition into ammonia and sulfur trioxide:

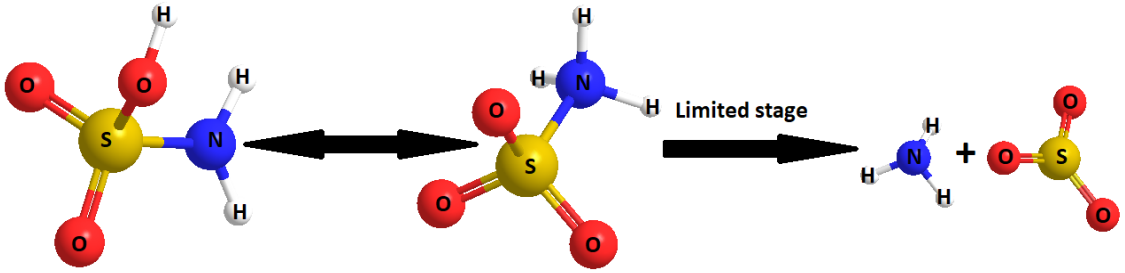

The increase in the reactivity of sulfamic acid in the presence of the main catalysts is explained by the formation of a donor – acceptor complex with a higher sulfation reactivity [32,33]. The rate of direct interaction of alcohols with sulfamic acid is lower than the rate of catalyzed sulfation, because the S – N bond in sulfamic acid is stronger than in the donor – acceptor complex [33].

In the study of starch sulfation by sulfamic acid the time and temperature of the process were varied. Data on the sulfur content in starch sulfate obtained under these experimental conditions is shown in table 1.

Table 1 Sulfur content of starch sulfate obtained by sulfamic acid-urea complex

№	Temperature, °C	Time, min	Sulfur content, mas. %
1	70	30	0,1
2	70	60	0,2
3	70	120	0,4
4	70	180	0,8
5	80	30	1,5
6	80	60	2,7
7	80	120	3,9
8	80	180	5,1
9	90	30	3,4
10	90	60	4,4
11	90	120	6,9
12	90	180	8,3
13	100	30	7,7
14	100	60	9,1
15	100	120	10,1
16	100	180	10,3

It was found that the sulfur content in sulfated starch can be controlled by varying the temperature and duration of the sulfation process (Table 1). The maximum sulfur content was

observed at a process temperature of 100°C and the time of process of 120 minutes. A further increase in the time of the process does not significantly affect the sulfur content in sulfated starch.

2. Kinetics of starch sulfation process

The kinetics of the starch sulfation process with a mixture of sulfamic acid - urea was studied in the temperature range 70–100 ° C. It was found that the starch sulfation process at all temperatures is satisfactorily described by a first-order equation (Fig. 1).

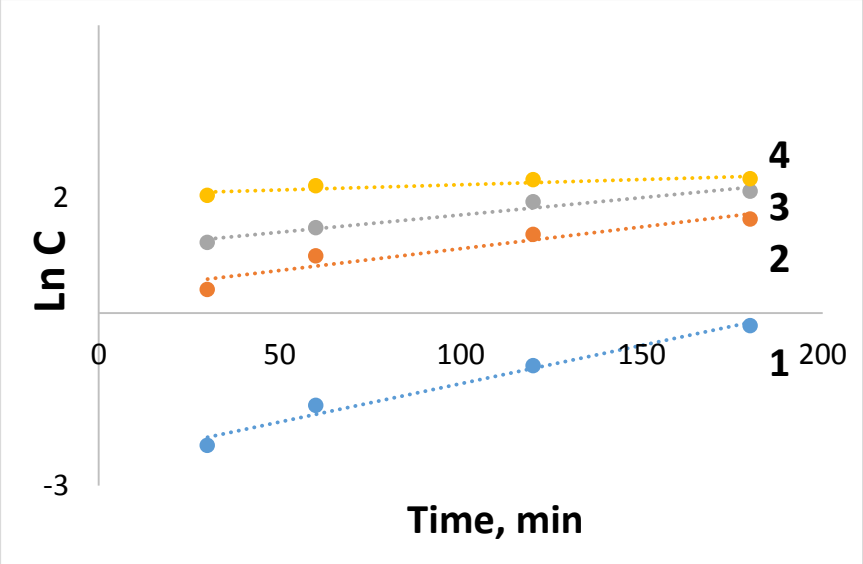

Fig. 1. Dependence of the logarithm of the sulfur content in sulfated starch (Ln C) on the duration of the sulfation process (1 - 70˚C, 2 - 80˚C, 3 - 90˚C, 4 - 100˚C)

The rate constants of the starch sulfation process were calculated from the change in sulfur content in sulfated starch. The activation energy of the sulfation process was determined from the temperature dependence of the rate constants in the Arrhenius coordinates (Fig. 2).

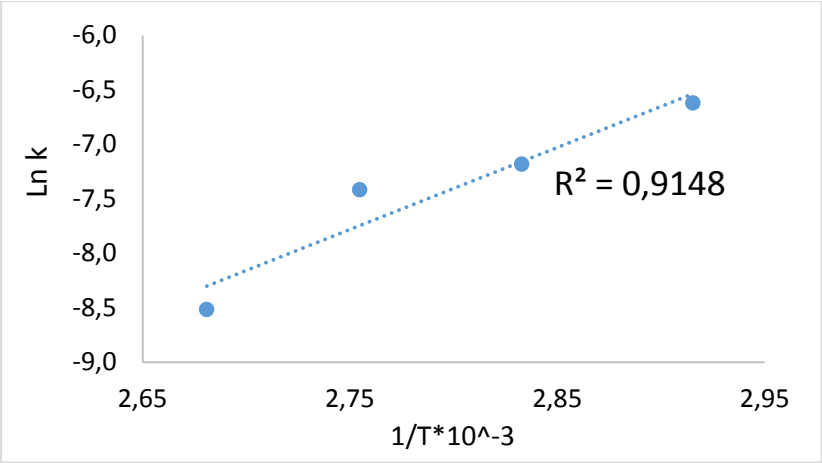

Fig. 2. Temperature dependence of the rate constants of starch sulfation process

As follows from the obtained results, the value of activation energy (E_a) for the process of solid-phase starch sulfation by sulfamic acid in the presence of urea is 64.1 kJ/mol.

3. Mathematical optimization of starch sulfation process

The aim of optimizing the sulfation process is to search for conditions that provide sulfated starch with a maximum sulfur content. The independent variables were used following factors: temperature (X_1) and the duration of sulphation process (X_2). The result of the sulfation process was characterized by the output parameter as the sulfur content in sulfated starch (Y_1).

Analysis of variance and mathematical modeling were performed for the output parameter (Y_1) of the starch sulfation process.

High prognostic properties of the mathematical model are also observed if it is implemented using the sulfur content in the sulfated starch sample as an output parameter (Table 2).

Table 2. Analysis of variance for Y_1 depending on X_1 and X_2

Variance source	Sum of squares	Number of degrees of freedom	Average square	F-Ratio	P-Value
A:X_1	51.0417	1	51.0417	134.88	0.0014
B:X_2	20.9067	1	20.9067	55.25	0.0050
AA	0.0938889	1	0.0938889	0.25	0.6526
AB	0.2025	1	0.2025	0.54	0.5174
BB	1.74222	1	1.74222	4.60	0.1212

Analysis of variance showed that, within the limits of the accepted experimental conditions, the factor X_1 makes a significant contribution to the total dispersion. This is indicated by the high values of the dispersion relations F, also called influence efficiencies. The influence of the dispersion source on the output parameter is considered statistically significant if the significance level is $P < 0.05$, corresponding to a confidence level of 95%.

The influence of factors X_1 and X_2 on the sulfur content (Y_1) in sulfated starch is described by the regression equation:

$$Y_1 = -9.1554-0.0668*X_1+0.086733*X_2+0.002167*X_1^2-0.0003*X_1*X_2-0.0001659*X_2^2 \quad (1)$$

The values of the output parameter Y_1 were compared with the values predicted by equation (1) (Fig. 3). The straight line corresponds to the calculated (predicted) values of Y1. The proximity of most "experimental points" to the straight line indicates that the selected model has good prognostic properties of the regression equations.

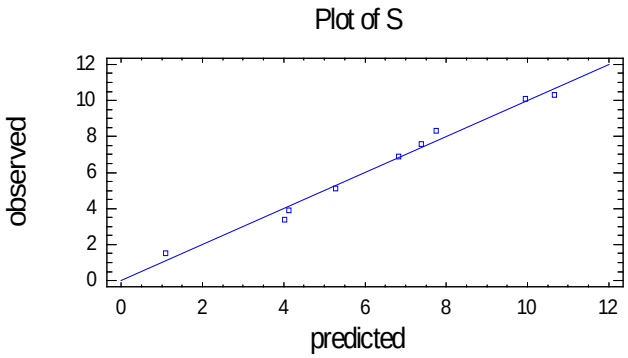

Fig. 3. Comparison of experimental and calculated values of sulfur content in sulfated starch during sulfation with varying time of process and temperature

Figure 4 shows the response surface of the output parameter Y_1 (sulfur content) temperature (X_1) and the time of the sulfation process (X_2).

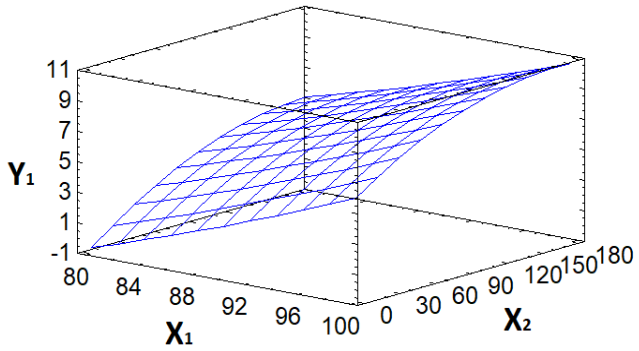

Fig. 4. The response surface of the output parameter Y_1 (sulfur content) and variable factors - X_1 and X_2

The optimal conditions for the starch sulfates obtaining with a maximum sulfur content (10.3% wt) are the process temperature of 99°C and a duration of 119 minutes.

4. The study of the structure of sulfated starch

4.1 FTIR spectroscopy

The inclusion of the sulfate group in the structure of starch was confirmed by FTIR spectroscopy (Fig. 5).

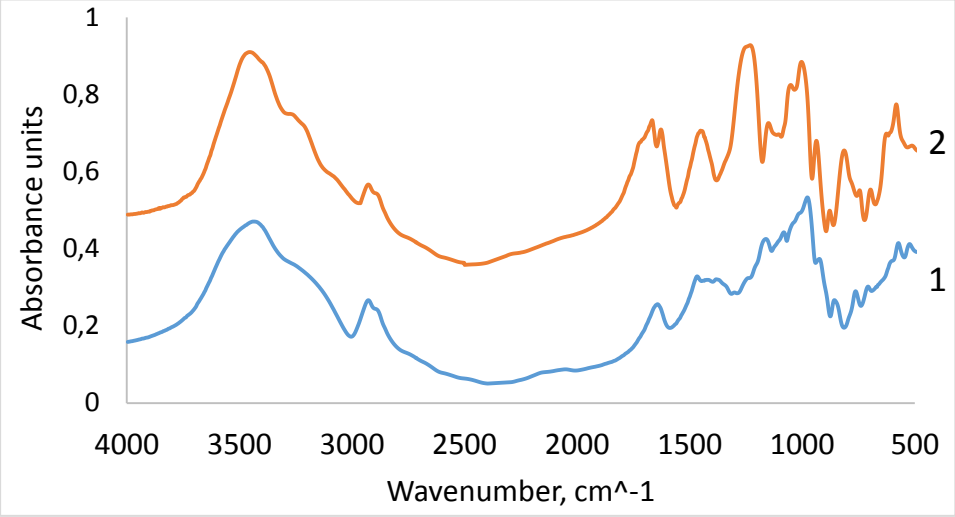

Fig.5. FTIR spectra of potato starch (1) and sodium salt of sulfated starch (2)

In the FTIR spectra of sulfated starch, in contrast to the original starch, there is a high-intensity band at 1255 cm^{-1}, which belongs to asymmetric stretching vibrations υ_{as} (O=S=O). The presence of absorption bands at 808–817 cm^{-1} and 859–867 cm^{-1}, which are absent in the FTIR spectrum of the initial starch, indicates the presence of primary and secondary sulfates of the sodium salt of starch (Fig. 5), which is consistent with the data presented in the works [36-38].

4.2 GPC analysis of sulfated starch

According to gel permeation chromatography (Fig.6,7), the initial starch has the main peak with Mn 139 kDa and Mw 382 kDa, and the molecular weight spread is quite large, individual molecules probably have a mass of more than 3000 kDa. Also in the sample there

is some admixture of oligosaccharides with a mass of about 1-2 kDa, probably formed as a result of partial hydrolysis of starch. In a sample of sulfated starch, the molecular weight distribution pattern changes significantly.

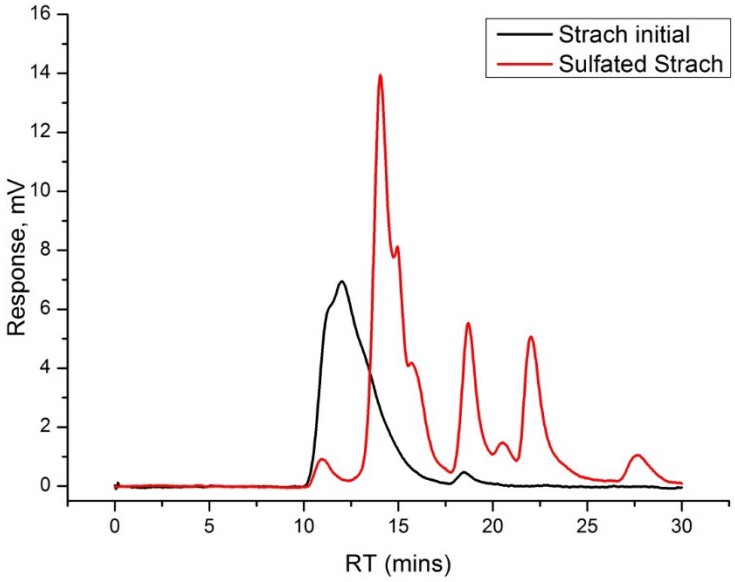

Fig. 6. Gel chromatogram of starch and sulfated starch samples

The peak with maximum mass (RT ~ 11min) most likely belongs to unreacted initial starch (Fig.6). The main peak with Mn 44kDa and Mw 60kDa refers to the target product. Moreover, in this area, three peaks can be distinguished, which can correspond to individual products of joint destruction and sulfation.

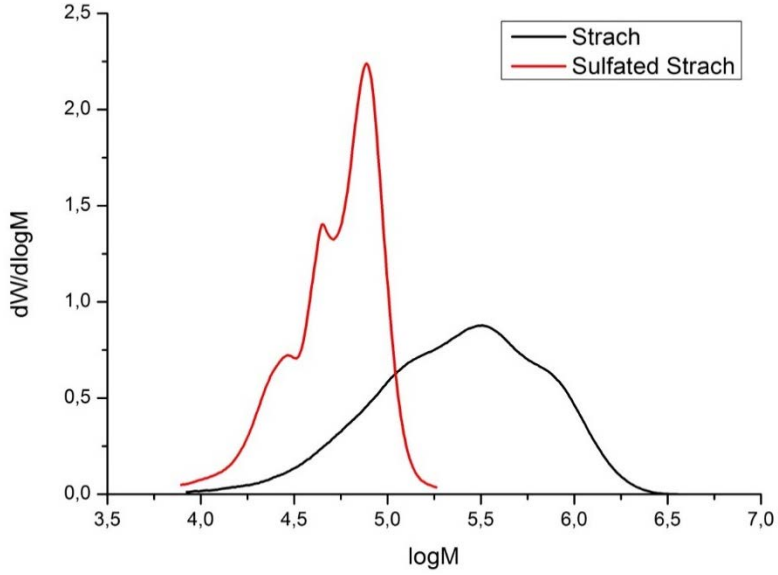

Fig.7. Curves of molecular weight distribution of the main peaks (samples of the initial starch and sulfated starch)

Also, this molecular weight distribution may indicate some fractionation of starch and probably different reactivity of individual sections of starch chains (Fig.7). The remaining

peaks with a release time of more than 17 minutes and a mass of less than 1 kDa relate to low molecular weight decomposition products of starch and their interaction with sulfamic acid and urea.

5. DFT calculation of starch sulfate

5.1. Molecular geometry

The first task for a computational study is to determine the optimized geometry of the molecule. Therefore, the optimized geometry of starch and sulfated starches were calculated using the B3LYP/6-31+G (d,p) method. The optimized molecular geometry in conformity with the atomic labeling of starch (a) and sulfated starches (b-d) are shown in Fig. 8.

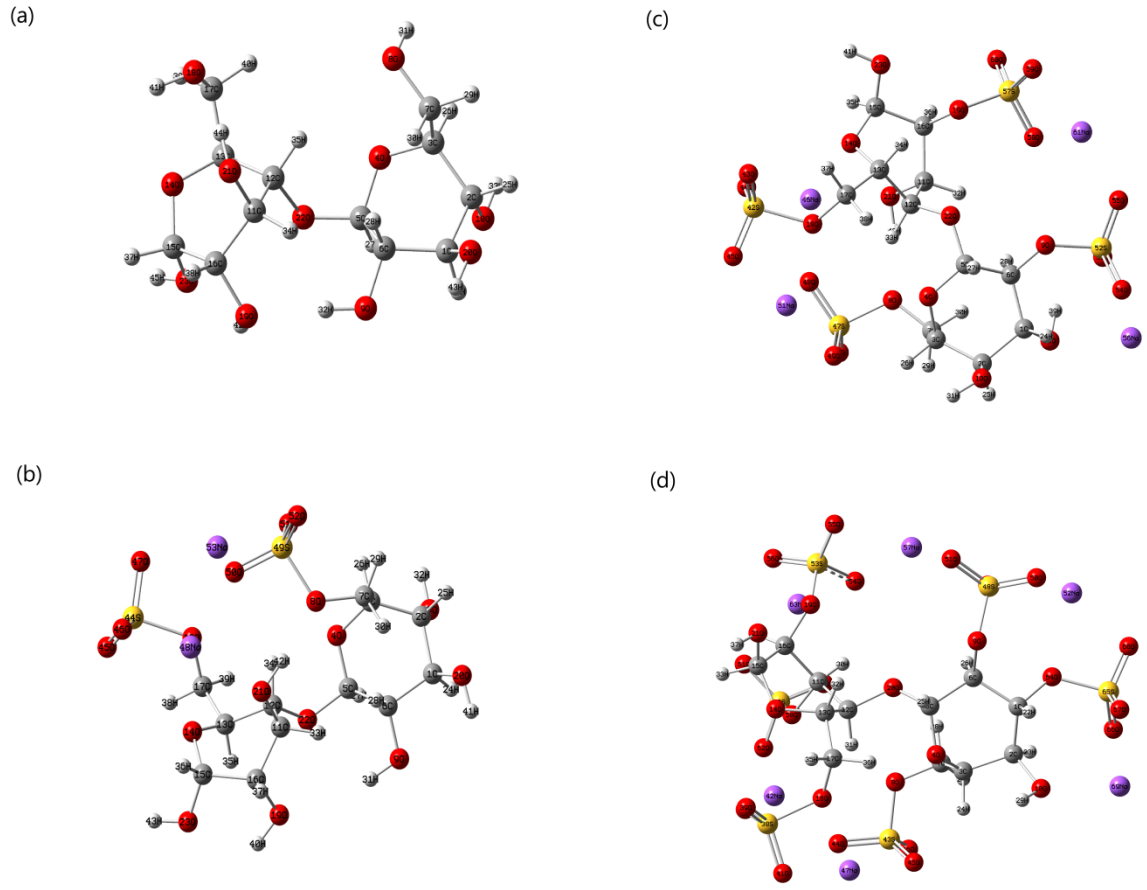

Fig. 8. The Optimized geometrical structures of starch (a), sulfated starch (b) sulfated starch (c) and sulfated starch (d) using B3LYP/6-31+G(d,p) level of theory.

The optimized structural parameters such as bond lengths and bond angles of starch and sulfated starches (b-d) are given in Table 3.

Table 3. Optimized bond lengths (Å) and bond angles (°) of starch and sulfated starch (C7 and C17) in gaseous phase

Parameters	Starch (a)	Parameters	Sulfated Starch (b) (C7 and C17)
Bond Lengths (Å)			
C1-C2	1.5393	C1-C2	1.5444
C1-C6	1.5347	C1-C6	1.5313
C1-O20	1.4283	C1-O20	1.4278
C1-H24	1.0965	C1-H24	1.0965
C2-C3	1.5374	C2-C3	1.538
C2-OO10	1.4323	C2-O10	1.4285
C2-H25	1.0981	C2-H25	1.0989
C3-O4	1.4326	C3-O4	1.4371
C3-C7	1.539	C3-C7	1.5503
C3-H26	1.1029	C3-H26	1.0936
O4-C5	1.4257	O4-C5	1.4127
C5-C6	1.5361	C5-C6	1.5319
C5-O22	1.4094	C5-O22	1.4266
C5-H27	1.0961	C5-H27	1.0966
C6-O9	1.4152	C6-O9	1.4186
C6-H28	1.0992	C6-H28	1.0973
C7-O8	1.4225	C7-O8	1.4421
C7-H29	1.1006	C7-H29	1.0954
C7-H30	1.0911	C7-H30	1.0915
O8-H31	0.9665	O8-S49	1.6875
O9-H32	0.9789	O9-H31	0.9705
O10-H33	0.9664	O10-H32	0.9668
C11-C12	1.5389	C11-C12	1.5563
C11-C16	1.5442	C11-C16	1.5299
C11-O21	1.4195	C11-O21	1.4378
C11-H34	1.0935	C11-H33	1.0927
C12-C13	1.5519	C12-C13	1.5429
C12-O22	1.4406	C12-O22	1.4293
C12-H35	1.0948	C12-H34	1.0905
C13-O14	1.4454	C13-O14	1.4454
C13-C17	1.5271	C13-C17	1.5211
C13-H36	1.0961	C13-H35	1.0957
O14-C15	1.4116	O14-C15	1.4195
C15-C16	1.5614	O14-O45	3.9865
C15-O23	1.4156	C15-C16	1.5499
C15-H37	1.0943	C15-O23	1.4083
C16-O19	1.4299	C15-H36	1.0953
C16-H38	1.0944	C16-O19	1.419
C17-O18	1.4321	C16-H37	1.0983
C17-H39	1.0968	C17-O18	1.4439
C17-H40	1.0929	C17-H38	1.0926
O18-H41	0.968	C17-H39	1.0947
O19-H42	0.9714	O18-S44	1.7546
O20-H43	0.9677	O19-H40	0.9693
O21-H44	0.9755	O20-H41	0.9677
O23-H45	0.9659	O21-H42	0.9761
		O23-H43	0.9675
		S44-O45	1.4611
		S44-O46	1.4855
		S44-O47	1.4862
		O46-Na48	2.2666
		S49-O50	1.4982
		S49-O51	1.4938
		S49-O52	1.4577
		O51-Na53	2.291
Bond Angles (°)			
C2-C1-C6	112.585	C2-C1-C6	112.1097

C2-C1-O20	107.9775	C2-C1-O20	108.0115
C2-C1-H24	106.8697	C2-C1-H24	106.9825
C6-C1-O20	111.1781	C6-C1-O20	110.7535
C6-C1-H24	107.7193	C6-C1-H24	108.3123
O20-C1-H24	110.4328	O20-C1-H24	110.617
C1-C2-C3	112.8948	C1-C2-C3	112.8118
C1-C2-O10	105.6116	C1-C2-O10	105.7784
C1-C2-H25	107.7448	C1-C2-H25	107.4446
C3-C2-OO10	110.6737	C3-C2-O10	110.7748
C3-C2-H25	109.3214	C3-C2-H25	109.2199
O10-C2-H25	110.5134	O10-C2-H25	110.7349
C2-C3-O4	112.4272	C2-C3-O4	111.8038
C2-C3-C7	112.9615	C2-C3-C7	111.3221
C2-C3-H26	107.6824	C2-C3-H26	109.3469
O4-C3-C7	112.1402	O4-C3-C7	113.3378
O4-C3-H26	104.2719	O4-C3-H26	103.3053
C7-C3-H26	106.6987	C7-C3-H26	107.2572
C3-O4-C5	118.9941	C3-O4-C5	119.3473
O4-C5-C6	111.343	O4-C5-C6	112.1888
O4-C5-O22	108.0437	O4-C5-O22	110.0167
O4-C5-H27	110.1606	O4-C5-H27	109.9062
C6-C5-O22	113.8316	C6-C5-O22	111.2545
C6-C5-H27	109.5638	C6-C5-H27	109.4985
O22-C5-H27	103.6109	O22-C5-H27	103.6359
C1-C6-C5	110.4641	C1-C6-C5	111.1458
C1-C6-O9	106.9902	C1-C6-O9	108.0765
C1-C6-H28	107.7097	C1-C6-H28	107.5691
C5-C6-O9	112.4914	C5-C6-O9	111.2659
C5-C6-H28	108.3802	C5-C6-H28	108.8633
O9-C6-H28	110.7056	O9-C6-H28	109.8464
C3-C7-O8	112.6453	C3-C7-O8	112.2187
C3-C7-H29	108.3248	C3-C7-H29	109.4742
C3-C7-H30	111.6301	C3-C7-H30	112.4622
O8-C7-H29	111.1407	O8-C7-H29	110.0415
O8-C7-H30	105.6548	O8-C7-H30	105.008
H29-C7-H30	107.3294	H29-C7-H30	107.4599
C7-O8-H31	109.3834	C7-O8-S49	117.7638
C6-O9-H32	110.533	C6-O9-H31	108.4185
C2-O10-H33	109.3737	C2-O10-H32	109.5012
C12-C11-C16	111.5171	C12-C11-C16	112.6369
C12-C11-O21	112.0876	C12-C11-O21	109.5675
C12-C11-H34	109.5565	C12-C11-H33	110.0035
C16-C11-O21	110.6291	C16-C11-O21	107.487
C16-C11-H34	106.0482	C16-C11-H33	107.271
O21-C11-H34	106.7032	O21-C11-H33	109.8034
C11-C12-C13	110.845	C11-C12-C13	110.8643
C11-C12-O22	111.4664	C11-C12-O22	115.3729
C11-C12-H35	109.7795	C11-C12-H34	106.5149
C13-C12-O22	105.557	C13-C12-O22	105.5587
C13-C12-H35	109.7096	C13-C12-H34	109.9309
O22-C12-H35	109.3955	O22-C12-H34	108.5569
C12-C13-O14	113.2036	C12-C13-O14	108.8061
C12-C13-C17	114.2454	C12-C13-C17	113.8295
C12-C13-H36	106.6299	C12-C13-H35	108.676
O14-C13-C17	104.4099	O14-C13-C17	107.3149
O14-C13-H36	109.4734	O14-C13-H35	109.7828
C17-C13-H36	108.7983	C17-C13-H35	108.386
C13-O14-C15	117.5159	C13-O14-C15	114.6585
O14-C15-C16	112.3548	C13-O14-O45	83.274
O14-C15-O23	111.9747	C15-O14-O45	153.4961

O14-C15-H37	103.6555	O14-C15-C16	112.5525
C16-C15-O23	107.9968	O14-C15-O23	112.0583
C16-C15-H37	110.705	O14-C15-H36	104.3043
O23-C15-H37	110.1394	C16-C15-O23	107.1331
C11-C16-C15	112.0609	C16-C15-H36	110.3033
C11-C16-O19	110.215	O23-C15-H36	110.5307
C11-C16-H38	106.3737	C11-C16-C15	109.7571
C15-C16-O19	112.3996	C11-C16-O19	106.0237
C15-C16-H38	108.0018	C11-C16-H37	109.3298
O19-C16-H38	107.4741	C15-C16-O19	112.9173
C13-C17-O18	112.1486	C15-C16-H37	108.226
C13-C17-H39	109.5232	O19-C16-H37	110.5399
C13-C17-H40	109.7464	C13-C17-O18	110.9423
O18-C17-H39	109.9681	C13-C17-H38	110.8098
O18-C17-H40	106.735	C13-C17-H39	109.0298
H39-C17-H40	108.6289	O18-C17-H38	109.1304
C17-O18-H41	107.138	O18-C17-H39	107.8921
C16-O19-H42	107.5934	H38-C17-H39	108.9676
C1-O20-H43	107.5653	C17-O18-S44	118.8977
C11-O21-H44	110.7435	C16-O19-H40	108.0867
C5-O22-C12	119.6042	C1-O20-H41	107.9778
C15-O23-H45	109.5559	C11-O21-H42	107.4257
		C5-O22-C12	119.3832
		C15-O23-H43	109.3681
		O18-S44-O45	106.3444
		O18-S44-O46	101.7765
		O18-S44-O47	98.0455
		O45-S44-O46	116.5704
		O45-S44-O47	117.13
		O46-S44-O47	113.4212
		O14-O45-S44	65.286
		S44-O46-Na48	108.4143
		O8-S49-O50	99.5548
		O8-S49-O51	105.4434
		O8-S49-O52	106.5802
		O50-S49-O51	110.1408
		O50-S49-O52	116.8299
		O51-S49-O52	116.1642
		S49-O51-Na53	98.4662

As seen from Table 3, the calculated bond lengths value of starch (a) are between 0.96 and 1.56 Å, whereas the bond lengths value of sulfated starch (b) are between 0.96 and 2.29 Å. In starch and sulfated starch, C15-C16 and O51-Na53 are the longest bonds, while O23-H45 and O10-H32 are the shortest bonds, respectively. C7-O8 and C17-O18 bond lengths in starch are calculated as 1.4225 and 1.4321 Å, whereas these bond lengths in sulfated starch are 1.4421 and 1.4439 Å. The shortening of bonding distance by sulfation can be explained by the fact that the atomic size of the sulfur is larger than hydrogen.

The calculated bond angles value of starch are between 103.61 and 119.60º, whereas the bond angles value of sulfated starch are between 65.28 and 119.38º. In starch and sulfated starch, C5-O22-C12 are the largest bond angles, while O22-C5-H27 and O14-O45-S44 are

the smallest bond angles, respectively. In starch, C5-O22-C12 with 119.60º bond angle decreased to 119.38 º by sulfation. In starch by sulfation, C3-O4-C5 with 118. 99º bond angle increased to 119.34 º, whereas C13-O14-C15 with 117.51º bond angle decreased to 114.65º.

5.2. Molecular electrostatic potential

The MEP is as a significant tool and its surface maps can be can be used to visualize charge distributions and charge dependent properties and to predict the electrophilic and nucleophilic attack regions of molecules [39,40]. The MEP surfaces of starch (a) and sulfated starches (b-d) were determined using the B3LYP/6-31+G (d,p) method used in optimization of molecules. The designated three-dimensional surface maps are shown in Fig. 9.

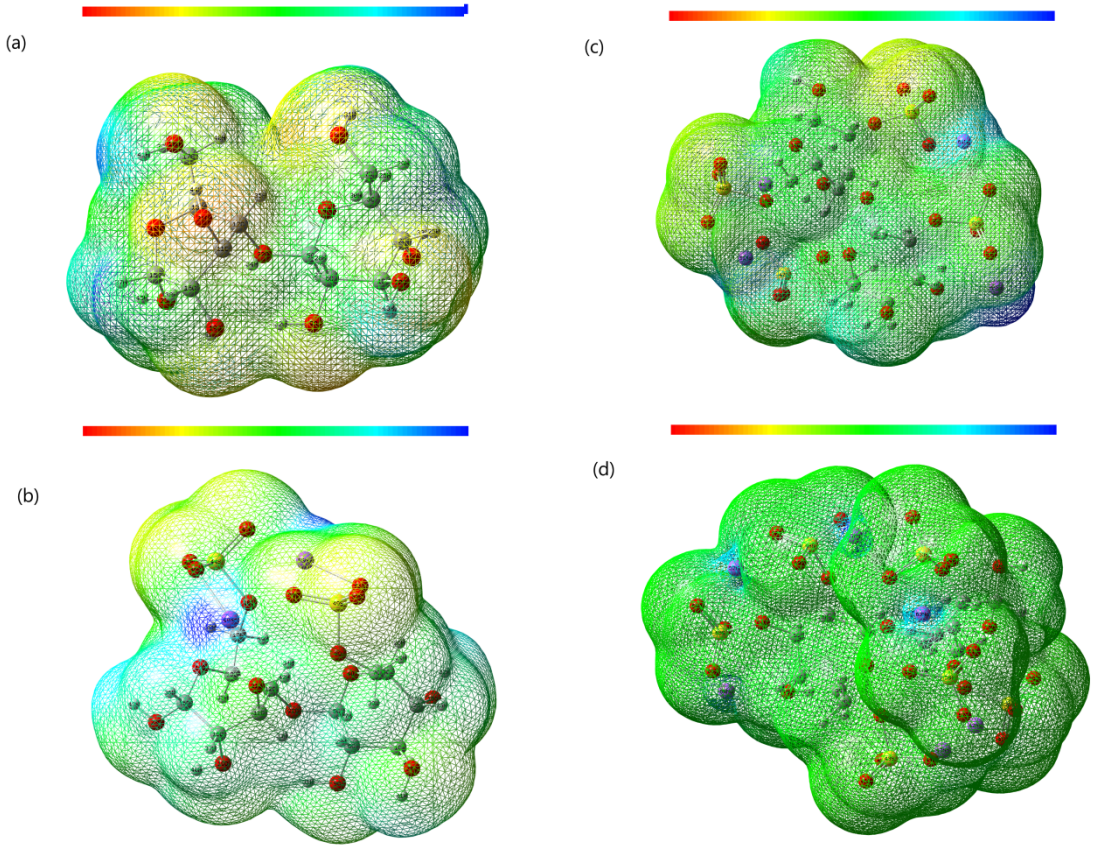

Fig. 9. Molecular electrostatic potential energy surface maps of starch (a), sulfated starch (b) sulfated starch (c) and sulfated starch (d) using B3LYP/6-31+G(d,p) level of theory.

In MEP analysis, the reactive regions can be seen with different color codes due to the color order of the electrostatic potential such as red <orange <yellow <green <blue. The blue color in the MEP maps represents the electron deficient region, which is the positive electrostatic potential, while the red color indicates the electron rich region, which is the

negative electrostatic potential. Besides, the green color in the MEP maps indicates the neutral region which is zero electrostatic potential.

As shown in Fig. 9 (a), the hydrogen atoms attached to oxygens have the lowest electron density and are shown as blue color on the map, while the electron density of the oxygen atoms is higher and is seen as reddish yellow. We noticed that the some changes in the MEP maps with the sulfation of starch. Looking at Fig. 9 (b-d), as the hydrogen atoms attached to the oxygen are sulfated, the blue color on the map is gradually diminished over hydrogen atoms due to the depletion of acidic hydrogens in starch molecule and finally positioned over the sodium atoms. Similarly, as the hydrogen atoms attached to the oxygen are sulfated, the electron density on oxygen atoms decreased and reddish yellow color shifted to green. Contour maps of MEP are drawn on the molecular plane and used to show electrostatic potential with constant density or bright lines. The contour maps of starch and sulfated starchs are demonstrated in Fig.10.

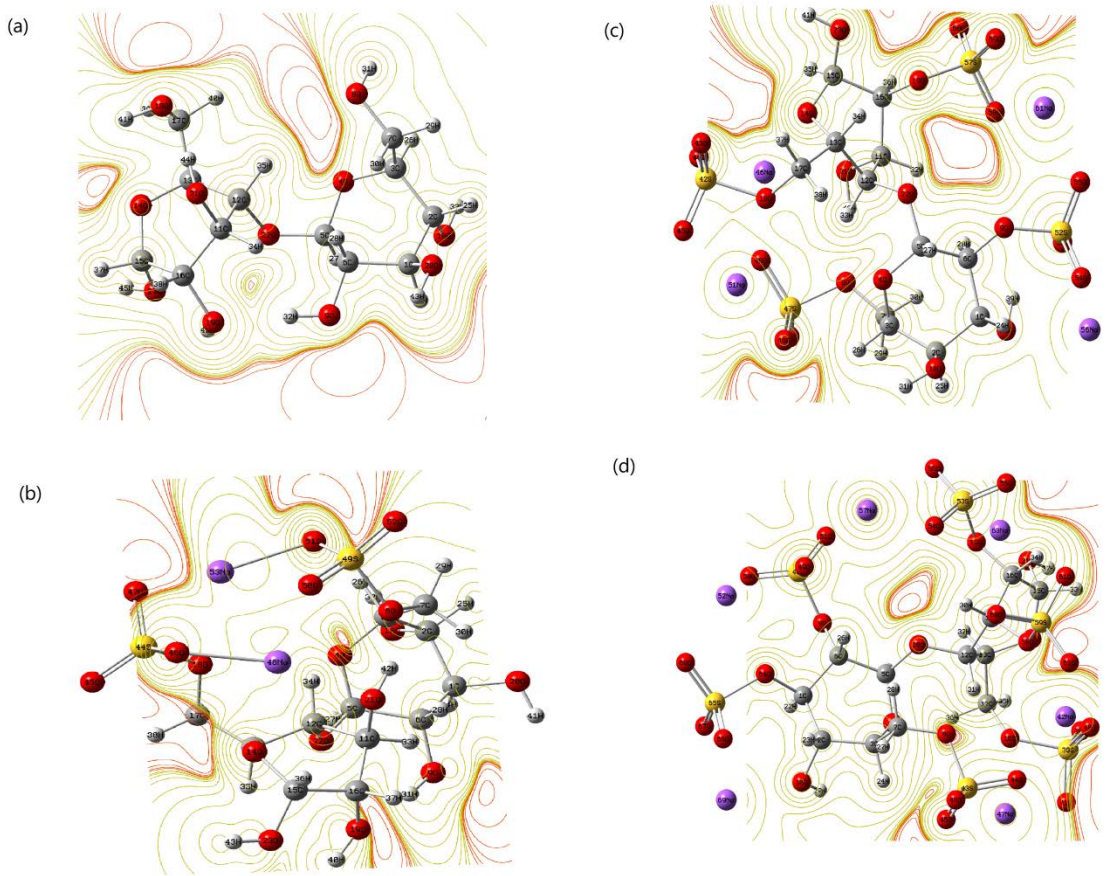

Fig. 10. The contour map of Molecular electrostatic potential surface of starch (a), sulfated starch (b) sulfated starch (c) and sulfated starch (d) using B3LYP/6-31+G(d,p) level of theory.

As shown in Fig.3, the contour maps of starch and sulfated starch demonstrate positive and negative potential regions relative to molecular electrostatic potential surfaces [41,42]. Here, yellowish lines which are electron-deficient zones or positive potential zones, while red lines are electron-rich zones or negative potential zones.

5.3. Frontier molecular orbital analysis

Frontier Molecular orbitals (HOMO and LUMO) and their energies (E_{HOMO} and E_{LUMO}) are very important for scientists, especially chemists and physicists, as in quantum chemistry. HOMO (Highest Occupied Molecular Orbital) and LUMO (Lowest Unoccupied Molecular Orbital) are called as Frontier molecular orbital (FMOs) because they can determine how the molecule interacts with other species. HOMO can be identified as a nucleophile that gives an electron that acts as an electron donor, while LUMO can be defined as an electrophile that receives an electron from the nucleophile that acts as an electron acceptor [43]. A molecule having a small energy gap means highly polarized and mostly associated with high chemical reactivity and low kinetic stability. Graphs of frontier molecular orbitals (HOMO and LUMO) of starch (a) and sulfated starches (b-d) were calculated by the B3LYP/6-31+G (d,p) method used in the optaimization of molecules and are shown in Fig.11.

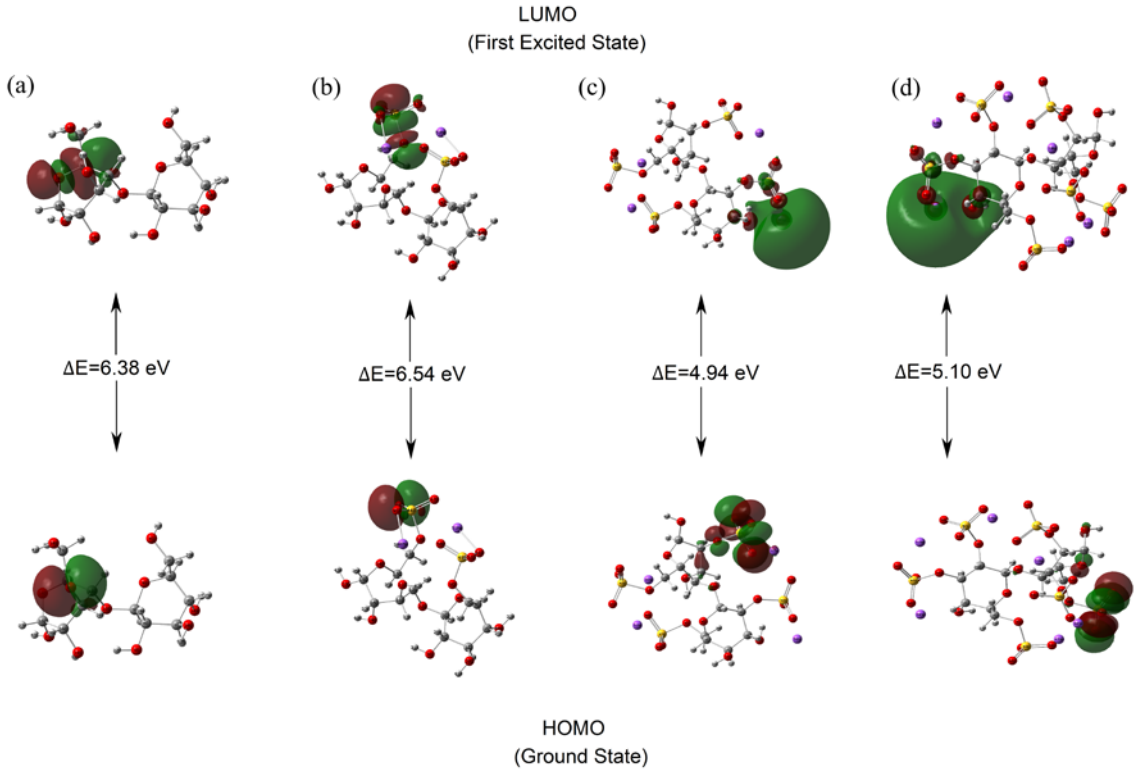

Fig. 11. Frontier molecular orbital (HOMO and LUMO) plots of starch (a), sulfated starch (b) sulfated starch (c) and sulfated starch (d) using B3LYP/6-31+G(d,p) level of theory.

As shown in Fig.11, HOMO and LUMO have nodes and are symmetrically located. Red is the positive phase, while green is the negative phase. Energy gap (Egap), Electronegativity (χ), electron affinity (EA), chemical potential (μ), ionization potential (IP), hardness (η), softness(ς), and electrophilicity index (ω) of starch and sulfated starches have been determined by using HOMO and LUMO energies and these descriptors can be calculated by the following equations [44,45]:

Energy gap (Egap); E_{gap}= $E_{LUMO} - E_{HOMO}$ (2)

Electronegativity; χ= $-{}^{1}/_{2}\,(E_{LUMO} + E_{HOMO})$ (3)

Electron affinity; $EA = -E_{LUMO}$ (4)

Chemical potential; μ = ${}^{1}/_{2}\,(E_{LUMO} + E_{HOMO})$ (5)

Ionization potential; $IP = -E_{HOMO}$ (6)

Hardness; η= ${}^{1}/_{2}\,(E_{LUMO} - E_{HOMO})$ (7)

Softness; $\varsigma = \frac{1}{\eta}$ (8)

Electrophilicity index; $\omega = \frac{\mu^2}{2\eta}$ (9)

The values of calculated descriptors are given in Table 4.

Table 4. Some electronic properties for starch and sulfated starches

Parameters (eV)	**Starch (a)**	**Sulfated Starch (b) (C7 and C17)**	**Sulfated Starch (c) (C6,C7 and C16,C17)**	**Sulfated Starch (d) (C1,C6,C7 and C11,C16,C17**
E_{HOMO}	-6.8950	-7.5283	-7.1748	-7.2583
E_{LUMO}	-0.5064	-0.9809	-2.2302	-2.1507
Energy Band Gap[$\Delta E = E_{LUMO} - E_{HOMO}$]	6.3886	6.5473	4.9445	5.1076

Electrophilicity index (ω)	2.1436	2.7647	4.4723	4.3332
Softness (ς)	0.3130	0.3054	0.4044	0.3915
Ionization energy (I)	6.8950	7.5283	7.1748	7.2583
Chemical potential (μ_o)	-3.7007	-4.2546	-4.7025	-4.7045
Dipole Moment (μ)	4.9122	5.1681	17.2591	17.1088
Electron affinity (A)	0.5064	0.9809	2.2302	2.1507
Electronegativity(χ)	3.7007	4.2546	4.7025	4.7045
Chemical hardness (η)	3.1943	3.2736	2.4722	2.5538
SCF Energy	-35320.2015	-78075.9469	-120830.0977	-163585.9201

As seen in Table 4, the chemical potential of starch and sulphated starches are negative values, ie the molecules are stable. In other words, they do not spontaneously decompose into elements. Hardness indicates the resistance of chemical systems to deformation of the electron cloud during chemical processing [46]. Hard systems having a large HOMO–LUMO energy gap are much less polarizable and relatively small, while soft systems having a small HOMO–LUMO energy gap are highly polarizable and large. Among the molecules studied, sulphated starch (b) has the highest energy gap and the lowest is sulphated starch (c). Sulphated starch (c) with an energy gap of 4.94 eV is more stable than the others, which means that easily charge transfer takes place easier than others. In addition, the sulfated starch (c) among the molecules studied had the highest dipole moment with a value of 17.25 D. As a result we can say that, the sulfated starch (c) is more polarizable than others and as the dipole moment is increased, the intermolecular interactions will increase.

5.4. Theoretical FTIR Analysis

The vibrational analysis for starch and sulfated starches were carried out by using DFT with B3LYP functional having extended 6-31+G (d,p) basis set. The calculated vibrational wavenumbers are generally higher than relevant experimental values due to the deficiencies of basis sets, electron correlation effects and calculations performed in the gaseous phase. Therefore, we used the scaling factor to match the theoretical results with the experimental data. The calculated frequencies are scaled by 0.9613 for DFT/B3LYP/6-31+G (d,p) computation [47]. The calculated FTIR spectra of starch and sulfated starches are shown in Fig. 12.

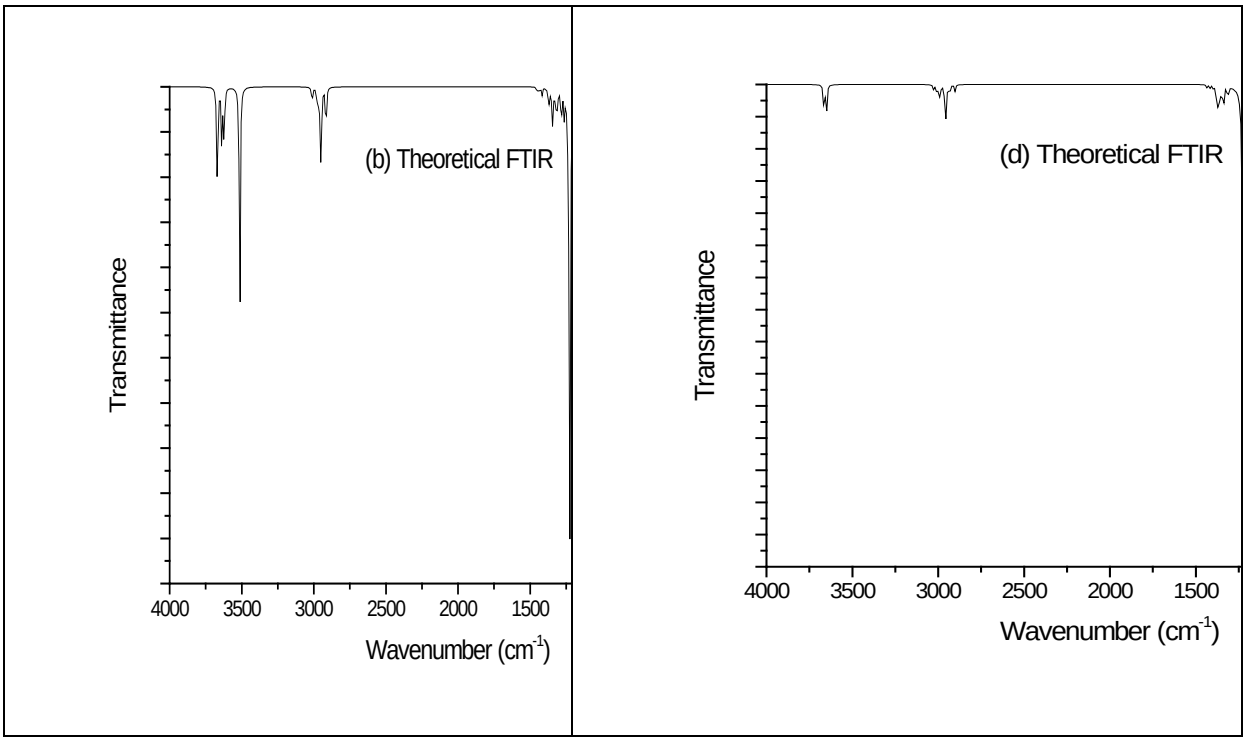

Fig. 12. The theoretical FTIR spectra of starch (a), sulfated starch (b), sulfated starch (c)and sulfated starch (d)using B3LYP/6-31+G(d,p) level of theory.

The selected important wavenumbers for sulfated starch are given Table 5. The theoretical FTIR spectra of starch (a) show that bands in the range of 3689-3446 cm^{-1} were related to -OH stretching vibrations which directly connected to the rings, while the bands at 3667 and 3661 cm^{-1} were related to -OH stretching vibrations adjacent to $-CH_2$ groups. The bands in the range of 3016-2860 cm^{-1} were related to -CH stretching vibrations. The bands at 1441 and 1442 cm^{-1} are related to the bending vibrations of $-CH_2$ groups adjacent to –OH. The band at 1126 cm^{-1} is related to the stretching vibrations of –COC. The theoretical FTIR spectra of sulfated starches (b-d) show that from b to d, as the hydroxyl groups are sulfated, the vibration bands of hydroxyl group gradually disappear and the signals of the sulfate groups arise. The bands in vicinity of 1201-1191 cm^{-1} are related to the asymmetric stretching vibrations of sulfate groups. As a result, the theoretical results are compatible with the experimental values.

Table 3. Selected important wavenumbers for sulfated starch as theroretically and experimentally

Major Assignments	**Vibrational Frequencies (cm^{-1})**	
	Theoretical	**Experimental**
ν O-H stretching (connected to ring)	3689-3446	3701-3381
ν O-H stretching (connected to $-CH_2$)	3667 and 3661	İn area 3701-3600*
ν C-H stretching	3016-2860	3006-2830

ν CH_2 (connected to –OH) stretching	1441 and 1442	1467 and 1423
ν C-O-C stretching	1126	1150
ν S-O stretching	1201 and 1191	1231

* - In this area, superposition of OH peaks of ν O-H stretching (connected to ring) and ν O-H stretching (connected to -CH_2)

5.5. Theoretical NMR Analysis

The theoretical chemical shifts for starch and sulfated starches were calculated by B3LYP method using 6-31+G (d,p) basis set with GIAO approach. The chemical shifts of ^{1}H NMR for starch (a) and sulfated starches(b-d) are listed in the Table 4. The ^{1}H NMR spectrum of starch (a) and sulfated starches(b-d) are shown in Fig. 13.

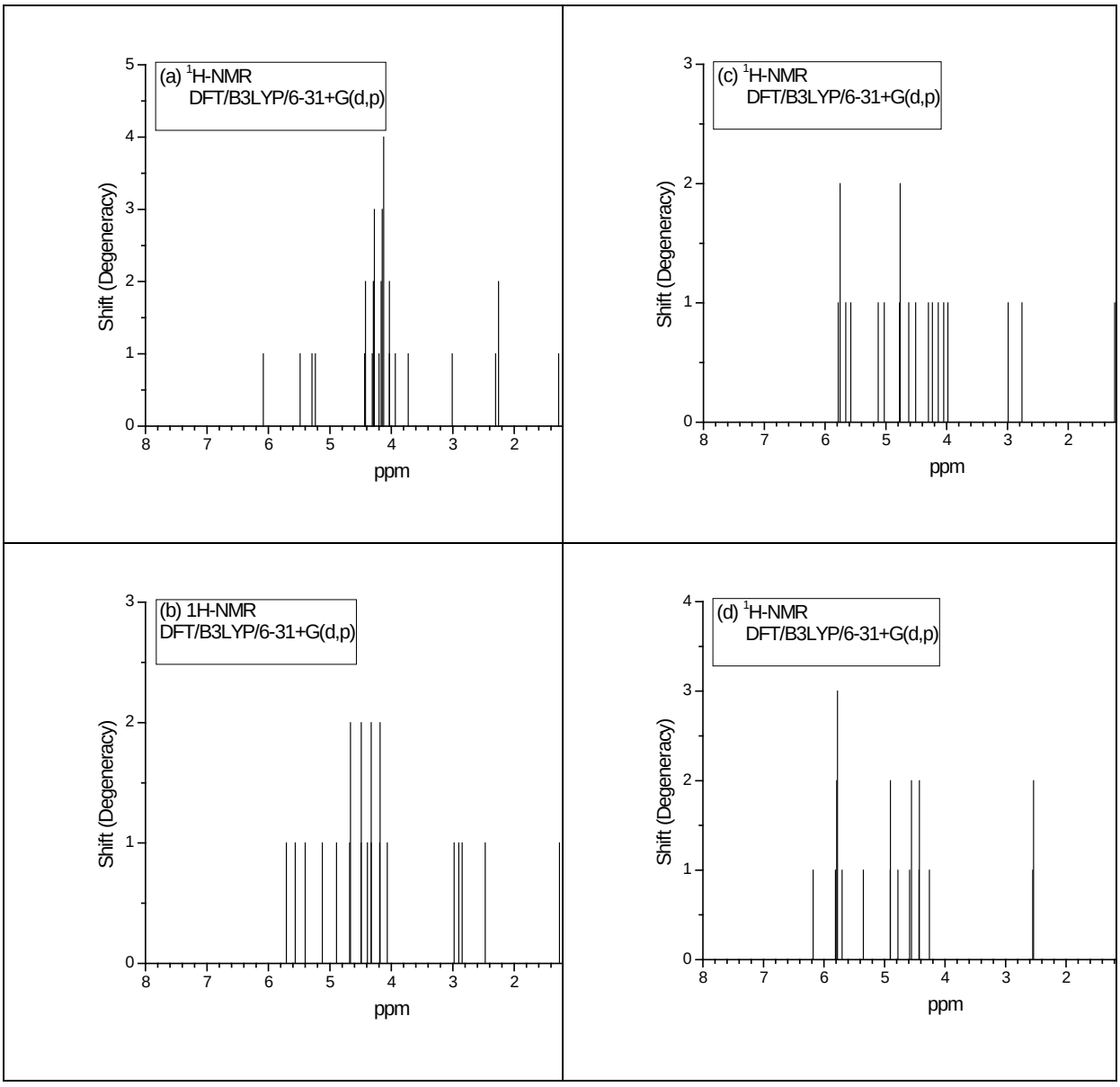

Figure 13. The theoretical ^{1}H NMR spectrum of starch (a), sulfated starch (b), sulfated starch (c)and sulfated starch (d)using B3LYP/6-31+G(d,p) level of theory.

As seen in Table 5, the hydrogens attached to O8 and O18 labeled atoms in starch (a) were disappeared by sulfation and the signals of the other hydrogens were altered in by the effect of sulfate group. In the same way, as the sulphation rate increases, the other hydrogens will disappear, as shown in Table 6.

Table 6. ^{1}H NMR chemical shifts for starch and sulfated starches

Starch (a)		**Sulfated Starch (b) (C7 and C17)**		**Sulfated Starch (c) (C6,C7 and C16,C17)**		**Sulfated Starch (d) (C1,C6,C7 and C11,C16,C17**	
Atoms	Values	Atoms	Values	Atoms	Values	Atoms	Values
37-H	6.0843	36-H	5.7086	35-H	5.7829	33-H	6.1776
27-H	5.4848	34-H	5.5626	33-H	5.7514	31-H	5.8117
32-H	5.2901	27-H	5.4021	27-H	5.6576	34-H	5.7891
35-H	5.2345	26-H	5.1217	26-H	5.5749	24-H	5.777
44-H	4.4338	38-H	4.8928	36-H	5.124	30-H	5.702
36-H	4.4212	37-H	4.679	37-H	5.0268	25-H	5.3483
38-H	4.3115	29-H	4.666	32-H	4.7742	35-H	4.9041
26-H	4.2912	39-H	4.4913	24-H	4.7654	26-H	4.9005
39-H	4.274	33-H	4.4886	29-H	4.6217	22-H	4.7789
28-H	4.1999	42-H	4.3901	38-H	4.5095	23-H	4.5838
25-H	4.1637	35-H	4.3284	28-H	4.3009	27-H	4.5537
34-H	4.1474	30-H	4.3256	34-H	4.2326	28-H	4.4304
29-H	4.123	28-H	4.1889	25-H	4.1367	36-H	4.4224
24-H	4.0318	25-H	4.1827	30-H	4.048	32-H	4.2597
30-H	4.0313	24-H	4.0666	40-H	3.9799	29-H	2.5506
40-H	3.936	40-H	2.9783	39-H	2.9875	37-H	2.5358
42-H	3.7251	43-H	2.9002	41-H	2.7597		
45-H	3.0093	31-H	2.8464	31-H	1.2352		
43-H	2.3038	41-H	2.4733				
41-H	2.254	32-H	1.2636				
33-H	1.2763						
31-H	0.9661						

In starch, the signals of two hydrogens attached to C7 and C17 labeled atoms adjacent to oxygens are shown at 4.03 and 4.12 ppm, but; in the sulfated starch, the two hydrogens attached to these carbon atoms shifted to low-field, ie ie a high chemical shift values of 4.32 and 4.66 ppm.

Conclusions

In the work, the possibility of solid-phase starch sulfation by sulfamic acid-urea complex has been established. This method of producing starch sulfates is simpler and environmentally friendly in comparison with known methods of sulfation.

To obtain starch sulfates with a high sulfur content (about 10 wt.%), It is advisable to carry out the sulfation process at a temperature of 100°C for 120 minutes.

The value of activation energy was calculated for the process of solid-phase sulfation of starch with sulfamic acid in the presence of urea, which amounted to 64.1 kJ/mol.

Mathematical modeling of the process of solid-phase starch sulfation by sulfamic acid-urea complex was carried out. The calculated conditions of the sulfation process providing the maximum sulfur content (10.3% wt) in sulfated starch are the process temperature of 99°C and a time of 119 minutes.

The inclusion of the sulfate group in the starch structure is confirmed by FTIR spectroscopy. In the FTIR spectra of sulfated starch, in comparison with the original starch, absorption bands appear at 1255 cm^{-1}, 808-817 cm^{-1} and 859-867 cm^{-1}, corresponding to vibrations of the sulfate group.

Initial starch and sulfated starch were analyzed by gel permeation chromatography. It has been shown that sulfated starch has a peak in the chromatogram relating to Mn 44kDa and Mw 60kDa.

Theoretical calculations of the starch and sulfated starches (in dimer forms) were performed using the DFT/B3LYP method with 6-31+G (d, p) basis set in the ground state. Optimized structural parameters such as bond lengths and bond angles were calculated and it was found that bond lengths and bond angles were reduced with the sulfating of starch. Nucleophilic and electrophilic attack regions of the the starch and sulfated starches were determined by molecular electrostatic potential and contour surface maps.

The HOMO and LUMO energy band gaps and other related molecular properties were computed and among the molecules studied, sulfated starch (c) with the lowest energy gap was found to be the most stable compound. Finally, FTIR and ^{1}H NMR analyzes of the starch and sulfated starches were performed and compared with each other. We hope that this study will be useful for those looking for theoretical and experimental evidence for starch and derivatives used in a variety of materials and applications.

Acknowledgements. The devices of the Krasnoyarsk Regional Centre for Collective Use of the SB RAS were used in the work. The authors are grateful to I.V. Korolkova for obtaining infrared spectra. For DFT calculations, the authors would like to thank Bingöl University for the server and Bitlis Eren University for supporting Gaussian 09W software.

Conflict of interest. There is no conflict of interest.

References

1. C.M. Dore, das C. Faustino, M.G. Alves, L.S. Will, T.G. Costa, D.A. Sabry, L.A. de Souza Rêgo, C.M. Accardo, H.A. Rocha, L.G. Filgueira, E.L. Leite. Carbohydrate Polymers 91 (2013) 467-475. doi: 10.1016/j.carbpol.2012.07.075

2. A.H.P. Gracher, A.G. Santana, T.R. Cipriani, M. Lacomini Carbohydrate Polymers 136 (2015) 177-186. DOI: 10.1016/j.carbpol.2015.09.022

3. R.C.R. Oliveira, R.R. Almeida, T.A. Gonçalves. J Dev Drugs., 5 (2016) 3 DOI: 10.4172/2329-6631.1000166

4. A.A. Kuzhim, N.N. Drozd, M.A. Torlopov, A.V. Il'ina. Eksp Klin Farmakol 76 (2013) 20-24.

5. D. Mihai, G. Mocanu, A. Carpov. European Polymer Journal, 37(3) (2001) 541–546. doi:10.1016/s0014-3057(00)00142-7

6. Y. Xu, Y. Wu, P. Sun, F. Zhang, R.J. Linhardt, A. Zhang. International Journal of Biological Macromolecules. 132 (2019) 970-977 doi:10.1016/j.ijbiomac.2019.03.213

7. G. Jiao, G. Yu, J. Zhang, H. Ewart. Marine Drugs. 9(2) (2011) 196–223. doi:10.3390/md9020196

8. H.E. Caputo, J.E. Strau, M.W. Grinsta ffChem. Soc. Rev. 48 (2019) 2338-2365. doi: 10.1039/c7cs00593h.

9. S.C. Zeeman, J. Kossmann, A.M. Smith. Annual Review of Plant Biology. 61(1) (2010) 209–234 doi: 10.1146/annurev-arplant-042809-112301.

10. D. Cui, M. Liu, L. Wu, Y. Bi. International Journal of Biological Macromolecules. 44 (2009) 294–299. DOI: 10.1016/j.ijbiomac.2009.01.003

11. N.N. Drozd, M.A. Torlopov, A.A. Kuzhim, V.A. Makarov. Eksp Klin Farmakol.75(6) (2012) 31-35.

12. A.A. Kuzhim, N.N. Drozd, M.A. Torlopov, V.A. Makarov. Hematology and Transfusiology (Rus.). 57(S3) (2012) 118-119.

13. H. Staroszczyk, M. Fiedorowicz, W.W. Zhong, P. Janas, P. Tomasik. e-Polymers, (2007). DOI:10.1515/epoly.2007.7.1.1635

14. P. Tomasik; C.H. Schilling. Adv. Carbohydr. Chem. Biochem. 59 (2004) 175-403. DOI: 10.1016/S0065-2318(04)59005-4

15. F. Schierbaum, K. Kordel. ACS Symposium Series. 77(11) (1978) 173–192. DOI: 10.1021/bk-1978-0077.ch011

16. K.B. Guiseley. ACS Symposium Series. 77(11) (1978) 148– 162. DOI: 10.1021/bk-1978-0077.ch009

17. Tessler M. (1978) U.S.Pat.4086419

18. D.W. Lim, H.S. Whang, K.J. Yoon, S.W. Ko. J. Appl.Polym.Sci.79 (2001) 1423–1430. https://doi.org/10.1002/1097-4628(20010222)79:8<1423::AID-APP90>3.0.CO;2-V

19. S. Geresh, A. Mamontov, J. Weinstein. J. Biochem. Biophys. Methods. 50 (2002) 179–187. DOI: 10.1016/s0165-022x(01)00185-3

20. A.F. Cirelli, J.A. Covian. Carbohydr. Res. 190(2) (1989) 329–337. DOI: 10.1016/0008-6215(89)84137-0

21. Whistler R.L. (1970). U.S. Pat. 3507855

22. M.L. Wolfrom, B.O. Juliano. J. Am. Chem. Soc. 82 (10) (1960) 2588–2592.

23. J.A. Sirviö, J. Ukkola, H. Liimatainen. Cellulose. 26(4) (2019) 2303–2316 doi:10.1007/s10570-019-02257-8

24. G. Lenteю Deterministic kinetics in chemistry and systems biology. Springer, New York. 2015.142 p. doi:10.1007/978-3-319-15482-4

25. I.G. Sudakova, N.V. Garyntseva, O.V. Yatsenkova, B.N. Kuznetsov Optimization of aspen wood delignification by H2O2 with sulfuric acid catalyst. J Sib Fed Univ Chem 6 (2013) 76–84

26. A.D. Becke. Phys. Rev. A. 38 (1988) 3098. doi:10.1103/PhysRevA.38.3098.

27. C. Lee, W. Yang, R.G. Parr. Phys. Rev. B.37 (1988) 785. doi:10.1103/PhysRevB. 37.785.

28. M.J. Frisch, G.W. Trucks, H.B. Schlegel, G.E. Scuseria, M.A. Robb, J.R. Cheeseman, G. Scalmani, V. Barone, B. Mennucci, G.A. Petersson, et al. Gaussian, Inc., Wallingford CT. 2010.

29. R. Dennington, T. Keith and J. Millam. GaussView, Version 5, Semichem Inc., Shawnee Mission KS. 2010.

30. R. Ditchfield J. Chem. Phys. 56 (1972) 5688.

31. P. Pulay J. Am. Chem. Soc. 112 (1990) 8251

32.V.A. Volkov, V.V. Suchkov. Sulfated nonionic surfactants (Rus). NITK. 1976. 65 p

33. N.Y. Vasil'eva, A.V. Levdansky, B.N. Kuznetsov, G.P. Skvortsova, A.S. Kazachenko, L. Djakovitch, C. Pinel. Russian Journal of Bioorganic Chemistry. 41(7) (2015) 725-731. DOI: 10.1134/S1068162015070158

34. R.A. Al-Horani, U.R. Desai. Tetrahedron. 66(16) (2010) 2907-2918. DOI: 10.1016/j.tet.2010.02.015

35. W. Spillane, J.B. Malaubier. Chemical Reviews. 114(4) (2014) 2507–2586. https://doi.org/10.1021/cr400230c

36. D. Cui, M. Liu, R. Liang, Y. Bi. Starch/Stärke. 59 (2007) 91–98. https://doi.org/10.1002/star.200600567

37. D. Cui, M. Liu, B. Zhang, H. Gong, Y. Bi. Starch/Stärke. 63 (2011) 354-363. doi:10.1002/star.201000033

38. H. Korva, J. Kärkkäinen, K. Lappalainen, M. Lajunen. Starch/Stärke. 68(9-10) (2016) 854-863. https://doi.org/10.1002/star.201600155

39. E. Scrocco, J. Tomasi. Adv. Quant. Chem. 11 (1978) 116-193.

40. J.S. Murray, K. Sen, Molecular Electrostatic Potentials, Concepts and Applications, Elsevier, Amsterdam, The Netherlands, 1996.

41. P. Demir, F. Akman. Journal of Molecular Structure. 1134 (2017) 404-415. https://doi.org/10.1016/j.molstruc.2016.12.101

42. E. Barim, F. Akman. Journal of Molecular Structure. 1195 (2019) 506-513 https://doi.org/10.1016/j.molstruc.2019.06.015

43. S. Muthu, S. Renuga, Spectrochim. Acta A 132 (2014) 313–325 https://doi.org/10.1016/j.saa.2014.05.009

44. R.G. Parr, R.A. Donnelly, M. Levy, W.E. Palke, J. Chem. Phys. 68 (1978) 3801–3807 https://doi.org/10.1063/1.436185

45. R.G. Parr, R.G. Pearson, J. Am. Chem. Soc. 105 (1983) 7512–7516. https://doi.org/10.1021/ja00364a005

46. A. Najiya, C.Y. Panicker, M. Sapnakumari, B. Narayana, B.K. Sarojini, C. Van Alsenoy. Spectrochimica Acta Part A: Molecular and Biomolecular Spectroscopy. 133 (2014) 526-533. DOI: 10.1016/j.saa.2014.06.049

47. J.B. Foresman. In Exploring chemistry with electronic structure methods: a guide to using gaussian. Edited by E. Frisch. Pittsburg, PA. 1996.